DELPHI Collaboration DELPHI 2002-08 CONF 549
March 4, 2002

Update at 202-209 GeV of the analysis of photon events with missing energy.

Preliminary

DELPHI Collaboration

E. Anashkin [1], **S. Ask** [2], **P. Checchia** [1], **A. De Min** [1], **V. Hedberg** [2], **S. Katsanevas** [3], **M. Margoni** [1], **C. Matteuzzi** [4], **F. Mazzucato** [1], **A. Perrotta** [5].

Abstract

An update of a study of the production of single and multi-photon events with missing energy has been made with the data collected at $\sqrt{s} = 202 - 209$ GeV with the DELPHI detector. The analysis uses a total integrated luminosity of 654 pb^{-1}. No excess of events beyond that expected from the Standard Model was observed and limits are set on new physics as described by supersymmetric models. A new limit on the gravitational scale is also determined.

Contributed Paper for Moriond'02

[1] Università e Sezione INFN, Padova, Italy.
[2] Lund University, Lund, Sweden.
[3] Université Claude Bernard de Lyon IPNL, Lyon, France.
[4] Università e Sezione INFN, Milano, Italy.
[5] Università e Sezione INFN, Bologna, Italy.

1 Introduction

At LEP2, the Standard Model predicts that events with one or more photons and invisible particles are produced exclusively by the reaction $e^+e^- \to \nu\bar{\nu}\gamma(\gamma)$ which receives a contribution from Z-exchange in the s-channel with single- or multi-photon emission from the initial state electrons and from the t-channel W exchange, with the photon(s) radiated from the beam electrons or the exchanged W.

Beyond the Standard Model, contributions to the γ + *missing energy* final state could come from a new generation of neutrinos, from the radiative production of some new particle, stable or unstable, weakly interacting or decaying into a photon. Theories of supersymmetry (SUSY) predict the existence of particles, such as the neutralino, which would produce a final state with missing energy and a photon if the lightest neutralino decays into $\tilde{G}\gamma$ with an essentially massless gravitino [1, 2] and several results have been published on the search for $e^+e^- \to \tilde{G}\tilde{\chi}_1^0 \to \tilde{G}\tilde{G}\gamma$ [3, 4]. If the gravitino is the only supersymmetric particle light enough to be produced, the expected cross-section for $e^+e^- \to \tilde{G}\tilde{G}\gamma$ can instead be used to set a lower limit on the gravitino mass [6]. Also in the same SUSY theoretical framework, multi-photon final states with missing energy could be a signature for neutralino pair-production, i.e. reactions of type $e^+e^- \to \tilde{\chi}_1^0\tilde{\chi}_1^0 \to \tilde{G}\gamma\tilde{G}\gamma$ [1, 2] and $e^+e^- \to \tilde{\chi}_2^0\tilde{\chi}_2^0 \to \tilde{\chi}_1^0\gamma\tilde{\chi}_1^0\gamma$ [7]. In the case of long neutralino lifetimes the photons would not originate at the beam interaction region and could have a large impact parameter. For mean decay paths comparable to the detector scale, events with a single photon not pointing to the interaction region are expected.

This paper describes the update of a study of the production of single and multi-photon events [4, 8] with 219 pb^{-1} of data collected by DELPHI during year 2000 at $\sqrt{s} = 202 - 209$ GeV. After a brief description of the selection criteria, a measurement of the number of neutrino families is made and limits on non-Standard Model physics, such as high-dimensional gravitons [9, 10] and supersymmetric particles, are presented. Since our latest conference contribution [5] a new reprocessing of the data has been used in the multi-photon analysis and new cross section limits and exclusion plots have been produced.

A more detailed description of the various detector components and the selection procedure is given in [4] and [8].

2 Event selection

2.1 Single-photon events

The general criteria for the selection of events are based mainly on the tracking system and the three electromagnetic calorimeters in DELPHI [11]: the STIC (in the very forward region), the FEMC (in the forward region) and the HPC (in the central region).

The basic selection criteria of events are: no charged tracks detected and no electromagnetic showers apart from the shower from the single photon candidate. Scintillation counters and silicon microvertex detectors were used to veto on charged particles. The details of the selection is described in [4].

2.2 Non-pointing single-photon events

The fine granularity of the HPC calorimeter provided a precise reconstruction of the axis direction in electromagnetic showers. This feature was used to select events with a single photon whose flight direction did not point to the beam interaction region. Events with a single non-pointing photon are expected when two neutral particles with large mean decay paths (> 4 m) are produced which subsequently decay into a photon and an invisible particle.

Events of this kind were searched for by requiring one photon in the HPC calorimeter with $E_\gamma > 10$ GeV and impact parameter exceeding 40 cm. Cosmic ray events, which represent the main experimental background, were largely reduced by vetoing on isolated hits or tracks in the Hermeticity Taggers and signals from the cathode-read-out system of the hadron calorimeter. More details on the precise event selection can be found in [8], where the analysis of the data samples collected at center-of-mass energies up to 183 GeV is described. The same analysis has been applied to the data sample taken at 189 GeV and published in [4] and an update of this analysis with the data recorded during 1999 and 2000 is presented in this paper.

2.3 Multi-photon events

A study of final states with at least two photons and missing energy with the 204-209 GeV data has also been made.

The physics motivations and the selection criteria have been discussed in detail in the two previously published papers [4, 8] dedicated to the analysis of the data taken at centre-of-mass energies up to 183 GeV and 189 GeV respectively. Here only a brief update of the results is given using the 2000 data and the same analysis method.

The selection of multi-photon final states was, as in the previously published analysis, based on a two-step procedure:

- In a first step all events with missing transverse energy and at least two photons, each with $x_\gamma > 0.05$ (where $x_\gamma = E_\gamma/E_{beam}$), were preselected. Very loose cuts on the polar angle of the photon and acoplanarity were adopted for the selection of this sample, which was used to monitor the modelling of the $e^+e^- \to \nu\nu\gamma\gamma(\gamma)$ process by the KORALZ 4.02 generator [13].

- In a second step these criteria were tightened in order to improve the experimental sensitivity for possible signals of supersymmetry, such as the $e^+e^- \to \tilde{\chi}^0_1\tilde{\chi}^0_1 \to \tilde{G}\gamma\tilde{G}\gamma$ or $e^+e^- \to \tilde{\chi}^0_2\tilde{\chi}^0_2 \to \tilde{\chi}^0_1\gamma\tilde{\chi}^0_1\gamma$ processes. This was achieved by imposing more stringent requirements on the photon polar angles as well as on the event missing mass and transverse momentum.

3 Comparison with the Standard Model expectations

3.1 Single-photon cross-section

The energy spectrum ($X_\gamma = E_\gamma/E_{beam}$) of the 1526 selected single photon events from all calorimeters is shown in Figure 1 together with the expected contributions from known sources. The X_γ distributions are shown for three $\sqrt{s}$-bins and the luminosity and average

$\sqrt{s}$ of the datasets that make up these bins are given in Table 1. The $\nu\bar{\nu}\gamma$ process was simulated by the KORALZ [13] program and then passed through the extensive detector simulation package of DELPHI [14]. The missing mass (or recoil mass) distributions of the events recorded at $\sqrt{s}$=181-209 GeV are shown in Figure 2. In this plot the distributions obtained with each of the three DELPHI electromagnetic calorimeters are shown separately. No sign of an excess above the Standard Model expectation is seen in either the highest energy data nor in any of the three calorimeter analysis.

The number of events and cross-sections obtained from the new event samples after correcting for background and efficiencies are given in Tables 2 and 3. The main source of background is the QED process $e^+e^- \to e^+e^-\gamma$ [15] where the two electrons escape undetected along the beampipe but also the contribution from other processes such as $\gamma\gamma$ collisions, $e^+e^- \to \gamma\gamma\gamma$, off-energy electrons [16], cosmic events, $e^+e^- \to \mu^+\mu^-\gamma$ and $e^+e^- \to \tau^+\tau^-\gamma$ have been estimated. The contribution from various sources to the systematic error amounts to $\pm$8%, $\pm$8% and $\pm$9% for the HPC, FEMC and STIC analysis respectively. The dominant uncertainty comes from the estimation of trigger and detection efficiencies.

Figure 3 shows the expected behaviour of the Standard Model single photon cross-section as a function of the LEP energy, compared with the values measured with all three DELPHI calorimeters. The new points at $\sqrt{s} = 202 - 209$ GeV are in agreement with the expectation of the Standard Model.

Averaging the three independent measurements done with the three different calorimeters at $\sqrt{s} = 181 - 209$ GeV, the number of light neutrino generations becomes:

$$N_\nu = 2.80 \pm 0.10(stat) \pm 0.14(syst)$$

3.2 Non-pointing single-photon events and multi-photon events

The numbers of events with a single non-pointing photon or with multi-photon final states found in the data sample at 204-209 GeV are compared to Standard Model expectations in Table 4.

The missing mass spectra for the preselected multi-photon events and the expected contribution from $e^+e^- \to \nu\overline{\nu}\gamma\gamma(\gamma)$ as simulated with KORALZ are shown in Figure 4. Additional background contributions from the processes $e^+e^- \to e^+e^-\gamma$ and $e^+e^- \to \gamma\gamma\gamma$ have been estimated to be 0.43$\pm$0.16 events at preselection level and have been added to the simulated sample. The measured missing mass distribution is in good agreement with the simulation.

No significant excess over Standard Model expectations was found in any of the data samples collected at energies up to $\sqrt{s} = 209$ GeV.

4 Limits on new phenomena

4.1 Limits on the production of unknown neutral states

4.1.1 Limits on $e^+e^- \to X\gamma$ production

The observed single photon events have been used to set a limit on the production cross-section of a new hypothetical particle, X, produced in association with a photon and being

stable or decaying to invisible decay products. Limits are calculated from the missing mass distribution (Figure 5) at $\sqrt{s} = 200 - 209$ GeV (average $\sqrt{s}$ =205.4 GeV) of the 414 single γ events in the angular region $12^\circ - 168^\circ$ and the 190 events in the angular region $45^\circ - 135^\circ$ while taking into account the expected background. The limit is valid when the intrinsic width of the X particle is negligible compared to the detector resolution (the recoil mass resolution varies between 10 GeV at the Z^0 peak to 1 GeV at high masses). The upper limit at the 95% confidence level of the cross-section for $e^+e^- \to \gamma$+X is given in Figure 5 for photons in the HPC region and in the FEMC+HPC region. In the latter case an assumption of an ISR-like photon angular distribution has been made to correct for losses between the calorimeters.

4.1.2 Limits on $e^+e^- \to XY \to YY\gamma$ production

A cross section limit has been calculated for the scenario where hypothetical X- and Y-particles are produced and the X-particle decays into a Y and a photon, $e^+e^- \to XY \to YY\gamma$. It is assumed that the Y particles escapes detection (such as in the process $e^+e^- \to \tilde{\chi}_2^0\tilde{\chi}_1^0 \to \tilde{\chi}_1^0\tilde{\chi}_1^0\gamma$ which is predicted by certain SUSY models) and that the branching ratio of $X \to Y\gamma$ is 100% .

It is, in addition, assumed that the E_γ- and $cos(\theta_\gamma)$-distributions are flat. This assumption results in a very small predicted signal within the STIC acceptance and for this reason only the single photon events recorded by the HPC and FEMC detectors were used in this analysis. Only the highest $\sqrt{s}$-bin (200-209 GeV) was used in the analysis and it was assumed that any $\sqrt{s}$-dependence of the signal would be insignificant in this limited $\sqrt{s}$-range. The analysis has been performed at 401 points in the mass plane of the X and Y particles where the selection cuts have been optimised in every point with a likelihood ratio method. The obtained and expected cross section limits, within the HPC + FEMC acceptance, in the mass plane of the X and Y particles are shown in figure 6.

4.2 Limits on the production of gravitons

If there are extra compact dimensions of space in which only gravity can propagate, gravitational interactions could be unified with gauge interactions already at the weak scale [9, 10]. The consequence of this model is that at LEP gravity could manifest itself by the production of gravitons (G), which themselves would be undetectable by the experiments. Instead single photons from the $e^+e^- \to \gamma G$ reaction are observable.

In these gravitational models, a fundamental mass scale, M_D, is introduced, which is related to the gravitational constant, the size of the compactified space and the number of dimensions, n, in addition to the usual 4 dimensional space. The differential cross-section for the $e^+e^- \to \gamma G$ process has been calculated by [10].

From Figure 2 it is clear that a very small signal can be expected in the STIC detector compared with the one in the FEMC and the HPC. For this reason only the two latter detectors were used in this analysis. All DELPHI data with $\sqrt{s} > 181$ GeV was used and for each bin in $\sqrt{s}$ (see Table 1) a limit was calculated after a cut optimization based on a likelihood ratio method [18]. These limits were then combined to give a cross-section limit at 95% C.L. and at 208 GeV of 0.14 pb for 2 and 4 extra dimensions. The resulting limits on the fundamental mass scale are $M_D > 1.36$ TeV for n=2 and $M_D > 0.84$ TeV for n=4 (Figure 7). This in turn translates into a limit on the size (radius) of the extra

dimensions wich is $R < 0.26$ mm and $R < 13$ pm for 2 and 4 extra dimensions. Limits for other numbers of extra dimensions are given in Table 5.

4.3 SUSY particles

4.3.1 Limits on the gravitino mass

The cross-section for the process $e^+e^- \to \tilde{G}\tilde{G}\gamma$ has been computed under the assumption that all other supersymmetric particles are too heavy to be produced [6] and lower limits on the mass of such a light gravitino has been extracted previously at LEP [3, 4]. The largest sensitivity is obtained with photons at low energy and/or low polar angle. Since the signal cross-section grows as the sixth power of the center-of-mass energy, the highest sensitivity is also found at the highest available beam energy.

After a combination in the same fashion as in the graviton analysis, a limit of $\sigma < 0.18$ pb at 95% C.L. and at 208 GeV was obtained by using the data at $\sqrt{s} = 181{-}209$ GeV from the FEMC and the HPC detectors. This corresponds to a lower limit on the gravitino mass which is

$$m_{\tilde{G}} > 1.12 \cdot 10^{-5} \text{ eV/c}^2 \quad \text{at 95\% C.L.}$$

while the expected limit is $1.14 \cdot 10^{-5}$ eV/c^2. Since the supersymmetry-breaking scale $|F|^{\frac{1}{2}}$ is related to the gravitino mass by $|F| = \sqrt{\frac{3}{8\pi}/G_N} \cdot m_{\tilde{G}}$, the limit on this scale is $|F|^{\frac{1}{2}} > 217$ GeV.

4.3.2 Limits on neutralino production if $\tilde{G}$ is the LSP

Supersymmetric models such as the gauge-mediated supersymmetric (GMSB) model [1] or the "no-scale" supergravity model (also known as the LNZ model) [2] predict that the gravitino $\tilde{G}$ is the lightest supersymmetric particle (LSP). If the next-to-lightest supersymmetric particle (NLSP) is the neutralino $\tilde{\chi}^0_1$, both single-photon and multi-photon production can occur at LEP2 via the processes $e^+e^- \to \tilde{G}\tilde{\chi}^0_1 \to \tilde{G}\tilde{G}\gamma$ and $e^+e^- \to \tilde{\chi}^0_1\tilde{\chi}^0_1 \to \tilde{G}\gamma\tilde{G}\gamma$. While the rate of the former process is proportional to the inverse of the gravitino mass squared, the di-photon process is independent of the gravitino mass. Consequently, the single-photon process is expected to dominate only for very light gravitinos.

The expected photon distributions from the process $e^+e^- \to \tilde{G}\tilde{\chi}^0_1 \to \tilde{G}\tilde{G}\gamma$ were generated with SUSYGEN [17], and the event selection was optimised with a likelihood ratio method. The same analysis was repeated at 26 different neutralino masses ($m_{\tilde{\chi}^0_1}$) between 80 and 208 GeV. The cross section limit for $e^+e^- \to \tilde{G}\tilde{\chi}^0_1 \to \tilde{G}\tilde{G}\gamma$ production was computed at 208 GeV and at a 95% C.L. after combining the limits from the the single photon data recorded with the FEMC and HPC detectors at a $\sqrt{s}$ between 181 and 209 GeV, assuming the signal cross-section to scale as β^8 (where β is the neutralino velocity).

The analysis was applied to two different theoretical scenarios. The first one was a more general scenario where the neutralino was assumed to be a pure bino and the right- and left-handed selectrons were degenerated in mass. Figure 8 shows the cross section limit within the FEMC + HPC acceptance assuming that the branching ratio $Br(\tilde{\chi}^0_1 \to \tilde{G}\gamma) = 100\%$. The exclusion regions in the $m_{\tilde{\chi}^0_1}$-$m_{\tilde{G}}$ mass plane are also depicted in Figure 8 for the selectron masses $m_{\tilde{e}} = 75$ GeV and $m_{\tilde{e}} = 150$ GeV.

The second scenario was the previously mentioned "no-scale" supergravity model where the selectron masses and the neutralino composition depend on the neutralino mass. This model also predicts a very light gravitino and the cross section limit and the exclusion region in the $m_{\tilde{\chi}_1^0}$-$m_{\tilde{G}}$ mass plane for this model can also be seen in Figure 8.

In the search for $e^+e^- \to \tilde{\chi}_1^0\tilde{\chi}_1^0 \to \tilde{G}\gamma\tilde{G}\gamma$ at $\sqrt{s}$ =204-209 GeV, 8 events were observed with 7.3 expected from Standard Model sources. This brings the total number of events found at $\sqrt{s}$ =130-209 GeV to 24 with 21 expected (Table 4). Figure 9 shows the cross-section limit [18] calculated from these events as a function of the $\tilde{\chi}_1^0$ mass (assuming a branching ratio of 100% for $\tilde{\chi}_1^0 \to \tilde{G}\gamma$) and the exclusion region in the $m_{\tilde{\chi}}$ versus $m_{\tilde{e}_R}$ plane. The dependence of the signal cross-section on the selectron mass is due to the possibility of t-channel selectron exchange in the production mechanism. As shown in Figure 9, a lower limit of 96 GeV/c^2 (100 GeV/c^2) at 95% C.L. for the χ_1^0 mass can be deduced with the hypotheses $m_{\tilde{e}_R} = m_{\tilde{e}_L} = 2m_{\tilde{\chi}}$ ($m_{\tilde{e}_R} = m_{\tilde{e}_L} = 1.1m_{\tilde{\chi}}$) and $\chi_1^0 \approx \tilde{B}$.

If the gravitino mass is larger than 200-300 eV/c^2, the $\tilde{\chi}_1^0$ can have such a long lifetime that it will decay far from the production point yet within the detector. The signature for this case is photons that do not point to the interaction region. If the decay length is long, the probability to detect both photons is small and therefore single photon events were searched for which had a shower axis reconstructed in the HPC which gave a beam crossing point at least 40 cm away from the interaction point [8]. 5 events were found at 202-209 GeV with 3 expected, bringing the total at all energies to 16 with 15 expected from Standard Model sources (Table 4).

Figure 10 shows the cross-section limit as a function of the mean decay path of the neutralino from the non-pointing single photon events.

4.3.3 Limits on neutralino production if $\tilde{\chi}_1^0$ is the LSP

In other SUSY models [7] the $\tilde{\chi}_1^0$ is the LSP and $\tilde{\chi}_2^0$ is the NLSP. The $e^+e^- \to \tilde{\chi}_2^0\tilde{\chi}_2^0 \to \tilde{\chi}_1^0\gamma\tilde{\chi}_1^0\gamma$ process has an experimental signature which is the same as for $e^+e^- \to \tilde{\chi}_1^0\tilde{\chi}_1^0 \to \tilde{G}\gamma\tilde{G}\gamma$ but with somewhat different kinematics due to the masses of the $\tilde{\chi}_1^0$ and $\tilde{\chi}_2^0$. The previous DELPHI analysis at lower energies [4, 8] has now been repeated with the 204-209 GeV data sample. Nine events remain after all cuts, with 8 expected from the Standard Model background (Table 4). Figure 11 shows the observed and expected cross-section limit calculated from the events collected at all energies as a function of the $\tilde{\chi}_1^0$ and $\tilde{\chi}_2^0$ masses, assuming a branching ratio of 100% for $\tilde{\chi}_2^0 \to \tilde{\chi}_1^0\gamma$.

5 Conclusions

An update of the analysis of single and multi-photon events with missing energy has been made with the 219 pb^{-1} of data collected by DELPHI in year 2000 at a center-of-mass energy between 202-209 GeV.

The measured single and multi photon cross-section is in agreement with the expectations from the Standard Model process $e^+e^- \to \nu\bar{\nu}\gamma(\gamma)$.

The absence of an excess of events has been used to set limits on the production of new unknown model-independent neutral states, a light gravitino and neutralinos. A new limit on the gravitational scale has also been determined.

References

[1] S. Dimopoulos *et al.*, Phys. Rev. Lett. **76** (1996) 3494;
S. Dimopoulos *et al.*, Nucl. Phys. **B488** (1997) 39;
S. Ambrosanio *et al.*, Phys. Rev. **D54** (1996) 5395;
S. Ambrosanio *et al.*, Phys. Rev. **D56** (1997) 1761.

[2] J. L. Lopez *et al.*, Phys. Rev. Lett. **77** (1996) 5168;
J. L. Lopez *et al.*, Phys. Rev. **D55** (1997) 5813.

[3] DELPHI Collaboration, P. Abreu *et al.*, Phys. Lett. **B380** (1996) 471;
DELPHI Collaboration, P. Abreu *et al.*, Eur. Phys. J. **C1** (1998) 1;
ALEPH Collaboration, R. Barate *et al.*, Phys. Lett. **B420** (1998) 127;
ALEPH Collaboration, R. Barate *et al.*, Phys. Lett. **B429** (1998) 201;
L3 Collaboration, M. Acciarri *et al.*, Phys. Lett. **B411** (1997) 373;
L3 Collaboration, M. Acciarri *et al.*, Phys. Lett. **B444** (1998) 503;
OPAL Collaboration, K. Ackerstaff *et al.*, Eur. Phys. J. **C2** (1998) 607;
OPAL Collaboration, K. Ackerstaff *et al.*, Eur. Phys. J. **C8** (1999) 23.

[4] DELPHI Collaboration, P. Abreu *et al.*, Eur. Phys. J. **C17** (2000) 53.

[5] "Update at 202-209 GeV of the analysis of photon events with missing energy"
DELPHI Collaboration, E. Anashkin *et al.*, DELPHI note 2001-082 CONF 510.

[6] A. Brignole, F. Feruglio and F. Zwirner, Nucl. Phys. **B516** (1998) 13;
A. Brignole, F. Feruglio and F. Zwirner, Erratum-ibid. **B555** (1999) 653.

[7] S. Ambrosanio and B. Mele, Phys. Rev. **D52** (1995) 3900;
S. Ambrosanio and B. Mele, Phys. Rev. **D53** (1996) 2541;
S. Ambrosanio *et al.*, Nucl. Phys. **B478** (1996) 46;
S. Ambrosanio and B. Mele, Phys. Rev. **D55** (1997) 1392;
G.L. Kane and G. Mahlon, Phys. Lett. **B408** (1997) 222.

[8] DELPHI Collaboration, P. Abreu *et al.*, Eur. Phys. J. **C6** (1999) 371.

[9] N. Arkani-Hamed, S. Dimopoulos and G. Dvali, Phys. Lett. **B429** (1998) 263.
E.A. Mirabelli, M. Perelstein and M.E. Peskin, Phys. Rev. Lett. **82** (1999) 2236.

[10] G.F. Giudice, R. Rattazzi and J.D. Wells, Nucl. Phys. **B544** (1999) 3.

[11] DELPHI Collaboration, P. Aarnio *et al.*, Nucl. Inst. and Meth. **A303** (1991) 233;
DELPHI Collaboration, P. Abreu *et al.*, Nucl. Inst. and Meth. **A378** (1996) 57.

[12] S.J. Alvsvaag *et al.*, Nucl. Inst. and Meth. **A425** (1999) 106.

[13] S. Jadach *et al.*, Comp. Phys. Comm. **66** (1991) 276;
S. Jadach *et al.*, Comp. Phys. Comm. **79** (1994) 503.

[14] DELPHI Collaboration, DELPHI 89-67 PROG 142;
DELPHI Collaboration, DELPHI 89-68 PROG 143.

[15] D. Karlen, Nucl. Phys. **B289** (1987) 23.

[16] E. Falk, V. Hedberg and G. von Holtey, CERN SL/97-04(EA).

[17] S. Katsanevas and P. Morawitz, Comp. Phys. Comm. **112** (1998) 227.

[18] A.L. Read, DELPHI 97-158 PHYS 737;
E Gross, A.L. Read and D. Lellouch, Proc. of "12^e Rencontres de Physique de la Vallée d'Aoste", M Greco INFN, Frascati, 1998 Frascati physics series 12 (599-628).

[19] J. L. Lopez and D.V. Nanopoulos, Phys. Rev. **D55** (1997) 4450.

[20] The CDF collaboration, F. Abe *et al.*, Phys. Rev. Lett. **81** (1998) 1791.

Year	$\sqrt{s}$ (GeV)		Luminosity (pb)		
	bin	average	HPC	FEMC	STIC
1997	180.8-184.0	182.7	50.2	49.2	51.4
1998	188.3-189.2	188.6	154.7	157.7	157.3
1999	191.4-191.8	191.6	25.9	25.9	25.9
1999	195.4-195.9	195.5	76.4	76.4	76.4
1999	199.1-200.0	199.5	83.4	83.4	83.4
1999	201.4-202.0	201.6	40.6	40.6	40.6
2000	202.0-204.5	203.7	8.4	8.4	8.4
2000	204.5-206.0	205.2	76.2	76.3	76.1
2000	206.0-207.5	206.7	121.6	125.7	125.6
2000	207.5-209.2	208.2	8.3	8.4	8.4

Table 1: The different datasets used in the single photon analysis.

	HPC	FEMC	STIC
$\sqrt{s}$:	202-209 GeV	202-209 GeV	202-209 GeV
θ_γ:	$45^\circ - 135^\circ$	$12^\circ - 32^\circ$, $148^\circ - 168^\circ$	$3.8^\circ - 8.0^\circ$, $172^\circ - 176.2^\circ$
x_γ:	> 0.06	> 0.1	> 0.3
$N_{observed}$:	161	178	101
$N_{background}$:	0.03	7.0	5.3
$N_{e^+e^-\to\nu\bar{\nu}\gamma}$:	170	166	95

Table 2: Number of selected and expected single photon events in the 2000 DELPHI data.

		203.7 GeV	205.2 GeV	206.7 GeV	208.2 GeV
STIC	σ_{meas} (pb)	1.78±1.10	1.44±0.23	1.08±0.16	1.19±0.63
$3.8° - 8°$	$\sigma_{\nu\bar{\nu}\gamma(\gamma)}$ (pb)	1.20	1.17	1.16	1.14
$172° - 176.2°$	N_ν	4.65±3.12	3.81±0.68	2.77±0.47	3.15±1.88
FEMC	σ_{meas} (pb)	1.67±0.61	1.64±0.22	1.70±0.17	1.15±0.55
$12° - 32°$	$\sigma_{\nu\bar{\nu}\gamma(\gamma)}$ (pb)	1.61	1.57	1.55	1.54
$148° - 168°$	N_ν	3.16±1.38	3.17±0.50	3.34±0.41	2.10±1.29
HPC	σ_{meas} (pb)	1.52±0.62	1.95±0.23	1.36±0.15	0.76±0.44
$45° - 135°$	$\sigma_{\nu\bar{\nu}\gamma(\gamma)}$ (pb)	1.64	1.62	1.59	1.58
	N_ν	2.69±1.64	3.89±0.62	2.37±0.42	0.70±1.22

Table 3: Measured and calculated cross-section with the three calorimeters for $e^+e^- \to \nu\bar{\nu}\gamma(\gamma)$ (KORALZ with three neutrino generations) and the number of neutrino generations calculated from the cross-sections.. The errors are statistical only.

	204-209 GeV		130-209 GeV	
	Observed	Expected	Observed	Expected
Preselected multi-photon events	18	19.8±0.6	68	64.6±1.3
$e^+e^- \to \tilde{\chi}_1^0\tilde{\chi}_1^0 \to \tilde{G}\gamma\tilde{G}\gamma$ selection	8	7.3±0.4	24	20.9±0.7
$e^+e^- \to \tilde{\chi}_2^0\tilde{\chi}_2^0 \to \tilde{\chi}_1^0\gamma\tilde{\chi}_1^0\gamma$ selection	9	7.9±0.4	26	23.8±0.8
Non-pointing single-photon events	5	3.0	16	14.6

Table 4: The number of observed and expected events from Standard Model sources in four selected data samples.

Dimensions	σ_{Limit} (pb)	M_D (expected)	M_D (obtained)	Radius
2	0.14	>1.32 TeV	>1.36 TeV	<0.26 mm
3	0.14	>1.01 TeV	>1.05 TeV	<3.3 nm
4	0.14	>0.82 TeV	>0.84 TeV	<13 pm
5	0.17	>0.69 TeV	>0.69 TeV	<0.48 pm
6	0.18	>0.59 TeV	>0.59 TeV	<54 fm

Table 5: Limits at the 95% confidence level on the fundamental mass scale M_D and the radius for different numbers of extra dimensions.

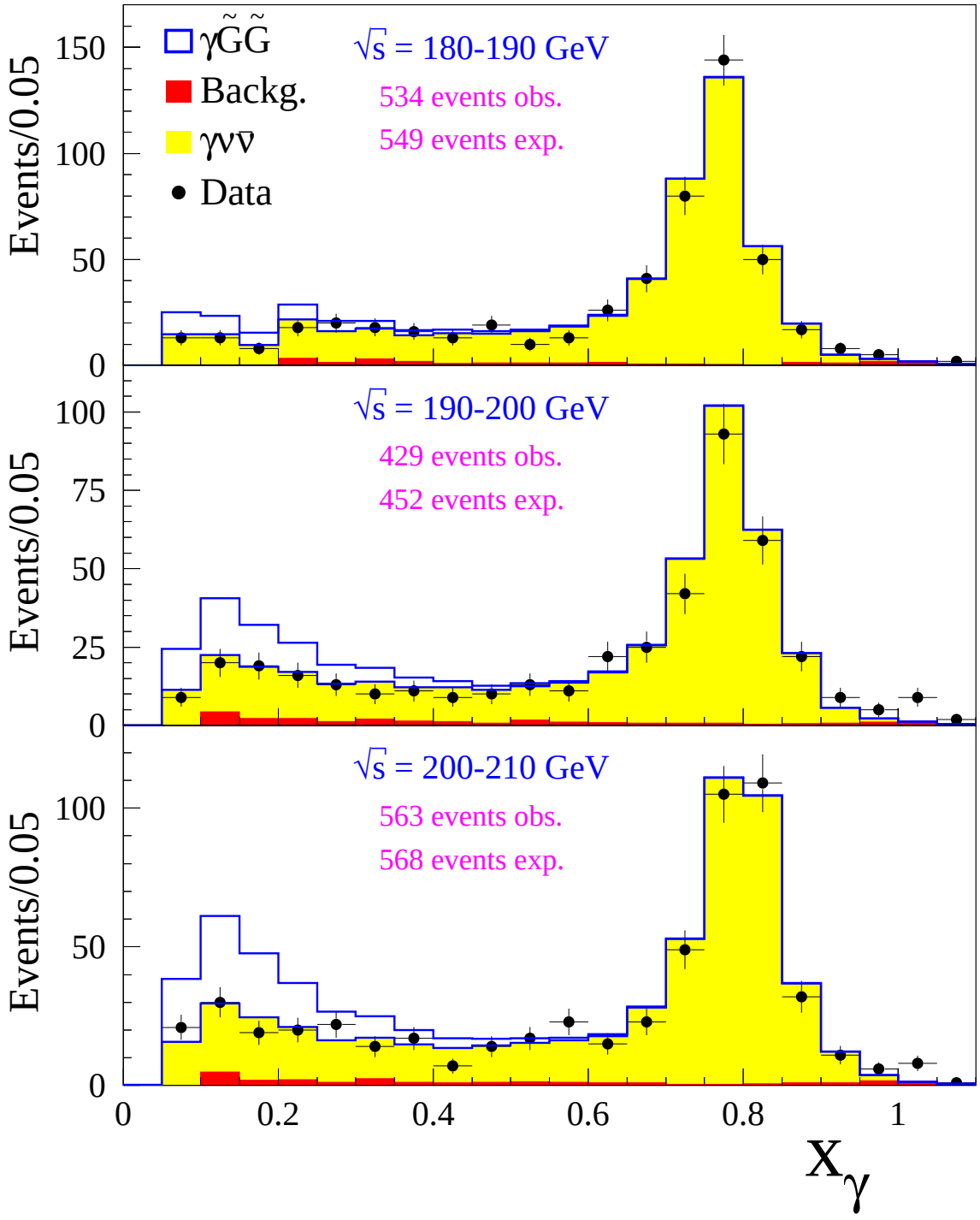

Figure 1: x_γ of selected single photons for three $\sqrt{s}$-bins. The light shaded area is the expected distribution from $e^+e^- \to \nu\bar{\nu}\gamma$ and the dark shaded area is the total background from other sources. Indicated in the plot is also the expected signal from $e^+e^- \to \tilde{G}\tilde{G}\gamma$ under the assumption that $m_{\tilde{G}} = 7 \cdot 10^{-6}$ eV/c^2.

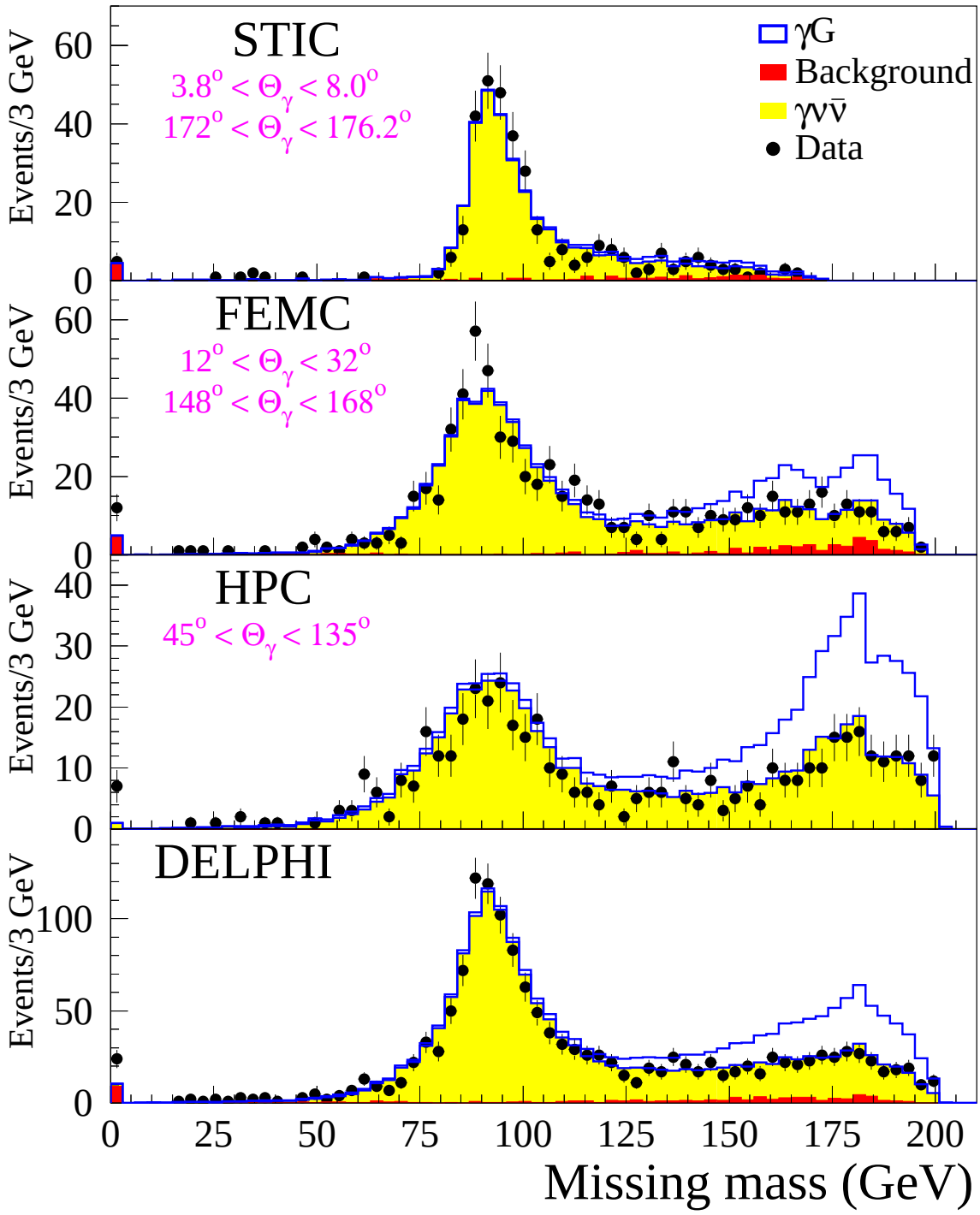

Figure 2: Missing mass (or recoil mass) distributions of all single photons in DELPHI (from data recorded at $\sqrt{s} = 181$-209 GeV). The figure shows the missing mass distribution from each calorimeter separately and the bottom plot shows the combined spectrum. The light shaded area is the expected distribution from $e^+e^- \to \nu\bar{\nu}\gamma$ and the dark shaded area is the total background from other sources. The expected signal from $e^+e^- \to \gamma G$ production is indicated (two extra dimensions and $M_D = 0.75$ TeV was assumed in this calculation).

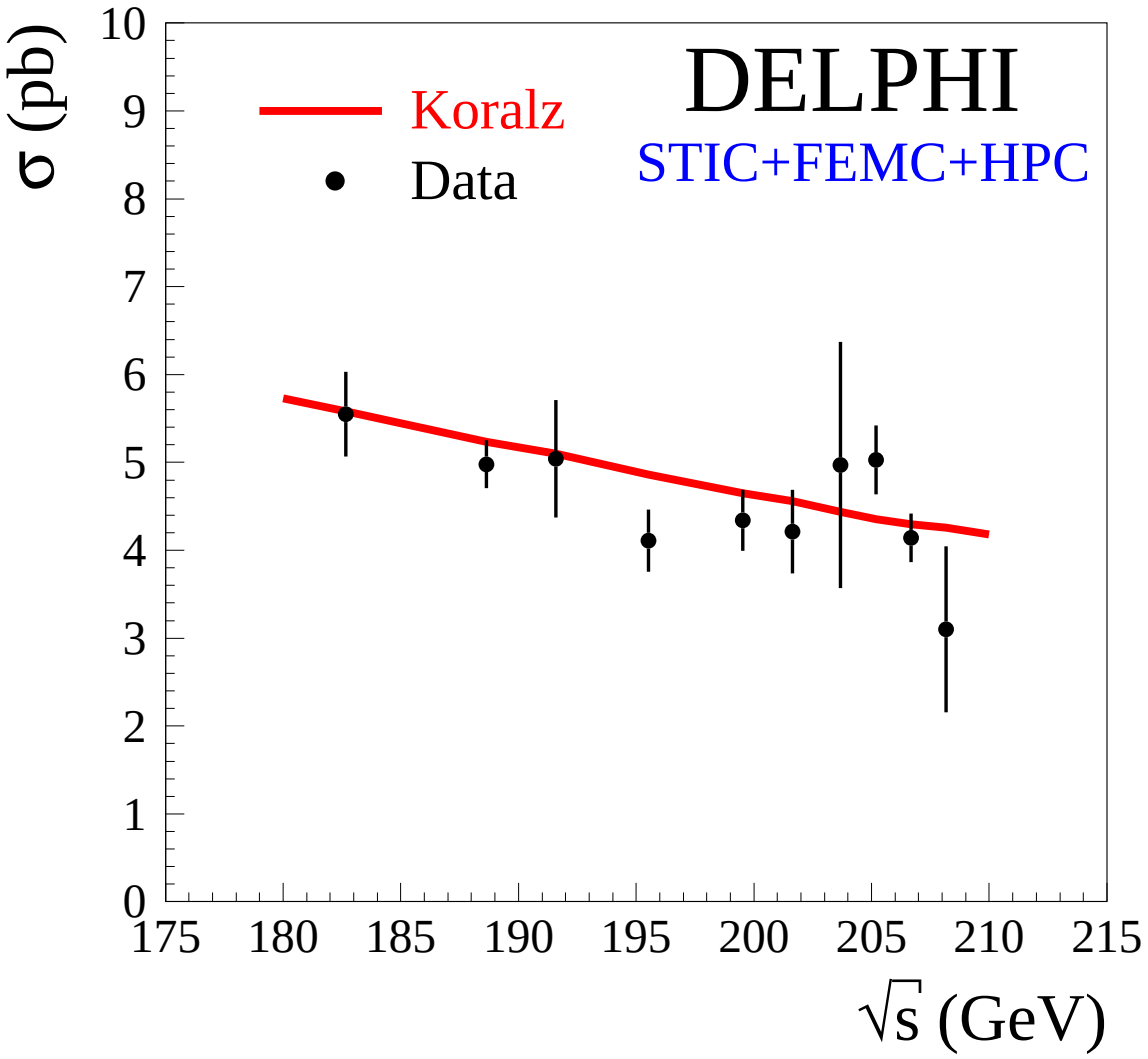

Figure 3: The single photon cross-section measured by the STIC, FEMC and HPC detector compared to the cross-section predicted by Koralz.

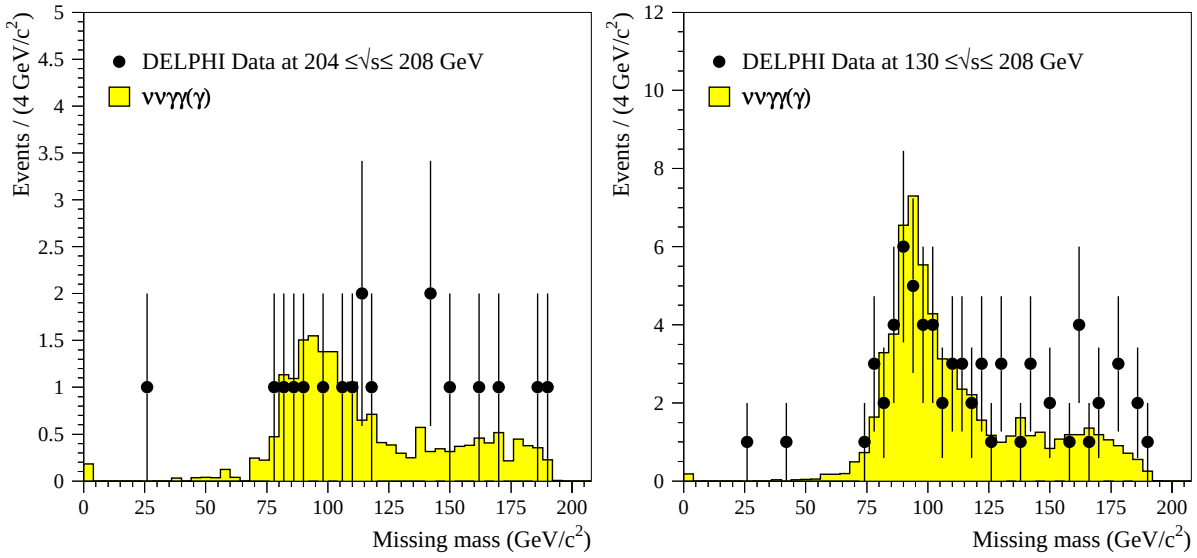

Figure 4: Missing mass distribution observed after multi-photon preselection in the 204-209 GeV sample (left) and the combined 130-209 GeV sample (right).

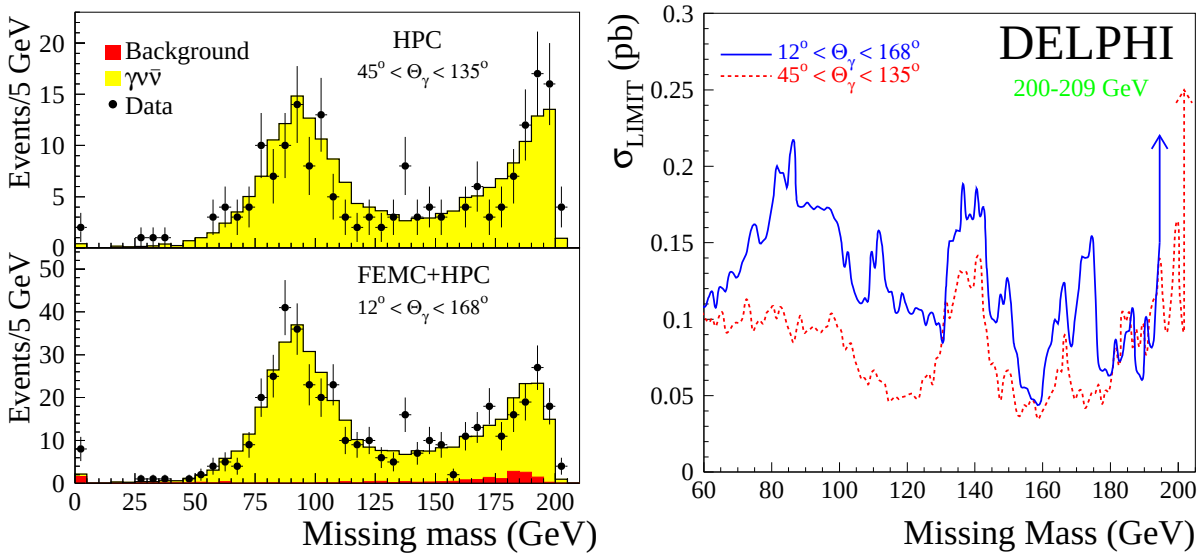

Figure 5: Left: The distributions of the missing mass for the events at 200-209 GeV in the HPC and in the FEMC+HPC. The light shaded area is the expected distribution from $e^+e^- \to \nu\bar{\nu}\gamma$ and the dark shaded area is the total background from other sources. Right: upper limit at 95% C.L. (within the solid angles described) for the production of a new unknown stable neutral object .

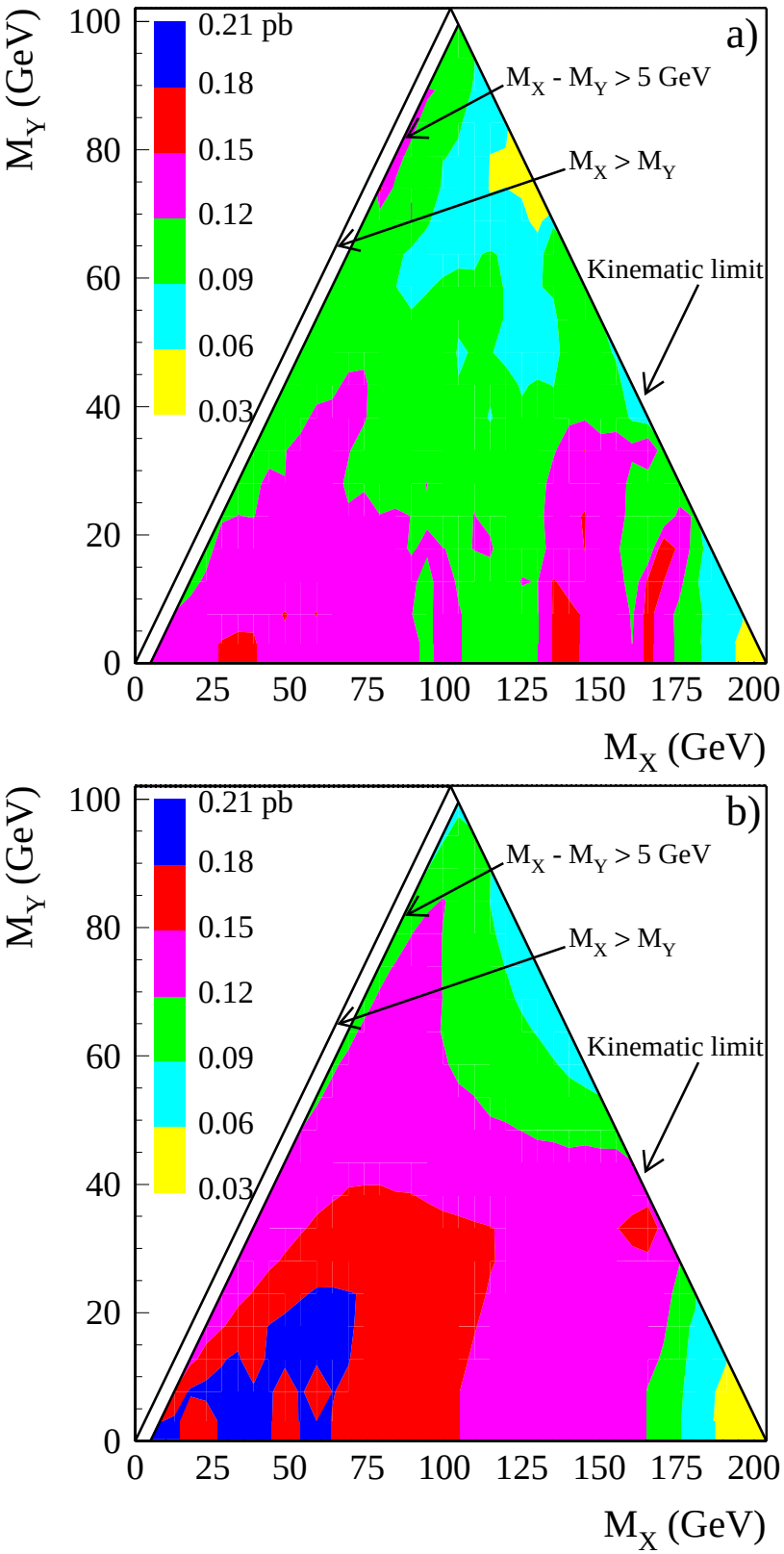

Figure 6: The obtained (a) and expected (b) cross section limit at 95% C.L. and at 205 GeV for the process $e^+e^- \to XY \to YY\gamma$ where X and Y are hypothetical new neutral particles.

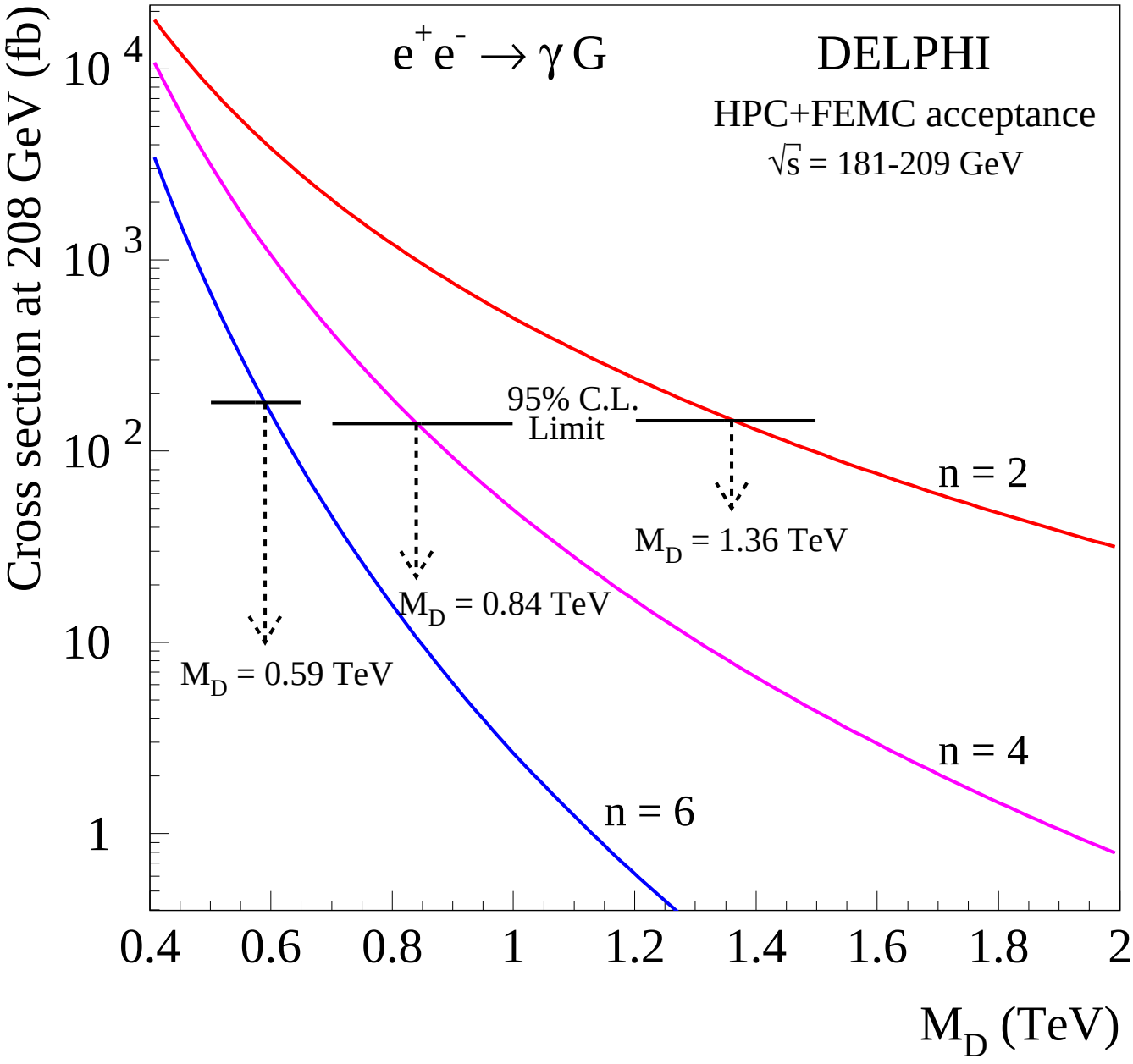

Figure 7: The cross-section limit at 95% C.L. for $e^+e^- \to \gamma G$ production at $\sqrt{s}$=208 GeV and the expected cross-section for 2, 4 and 6 extra dimensions.

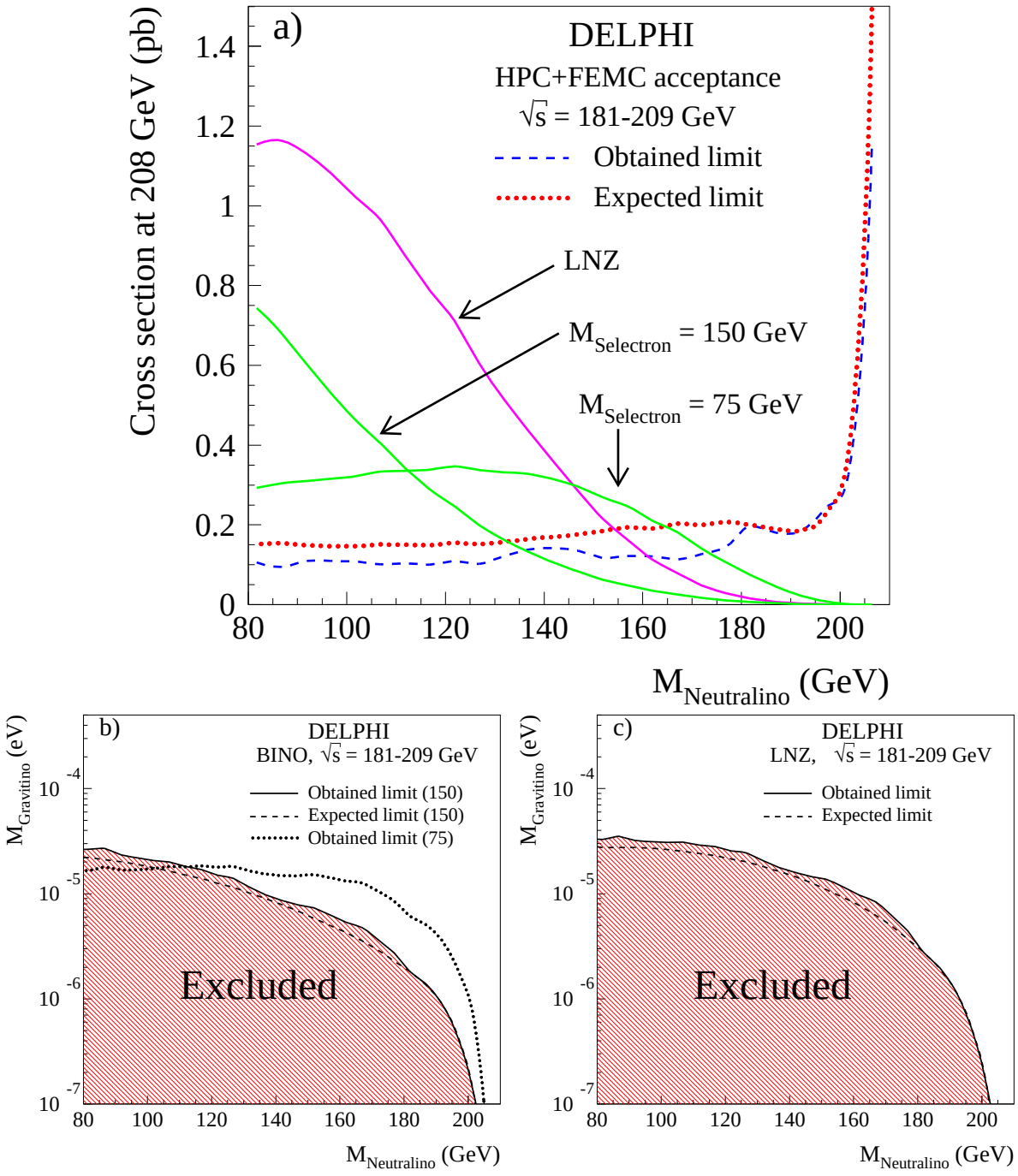

Figure 8: a) Cross section limit at 95% C.L. and at $\sqrt{s}$ =208 GeV of the process $e^+e^- \rightarrow \tilde{G}\tilde{\chi}_1^0 \rightarrow \tilde{G}\tilde{G}\gamma$ as a function of the $\tilde{\chi}_1^0$ mass. The predicted cross-sections under the assumption that the neutrino is a Bino or as described by the LNZ-model are also shown for $m_{\tilde{G}} = 1 \times 10^{-5}$ GeV. b), c) Exclusion plots in the $m_{\tilde{\chi}_1^0}$-$m_{\tilde{G}}$ mass plane.

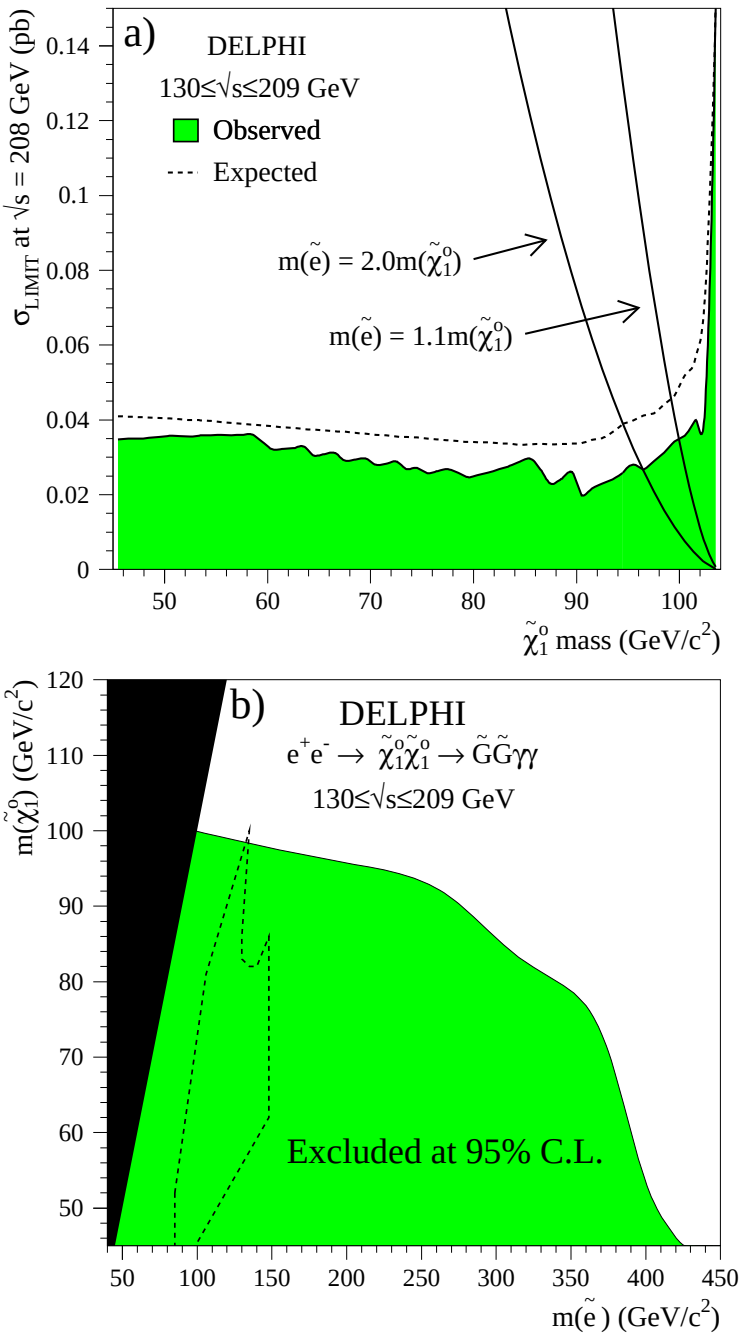

Figure 9: a) Upper limit at 95% C.L. on the cross-section at $\sqrt{s}$ =208 GeV of the process $e^+e^- \to \tilde{\chi}_1^0\tilde{\chi}_1^0 \to \tilde{G}\gamma\tilde{G}\gamma$ as a function of the $\tilde{\chi}_1^0$ mass and the predicted cross-section for two different assumptions for the selectron mass. The limit was obtained by combining all data taken at $\sqrt{s}$ =130-209 GeV, assuming the signal cross-section scales as β/s (where β is the neutralino velocity). b) The shaded area shows the exclusion region in the $m_{\tilde{\chi}}$ versus $m_{\tilde{e}_R}$ plane, calculated from the DELPHI data at $\sqrt{s}$ =130-209 GeV. The region compatible with the selectron interpretation [19] of the CDF ee$\gamma\gamma$ event [20] is shown by the dashed line.

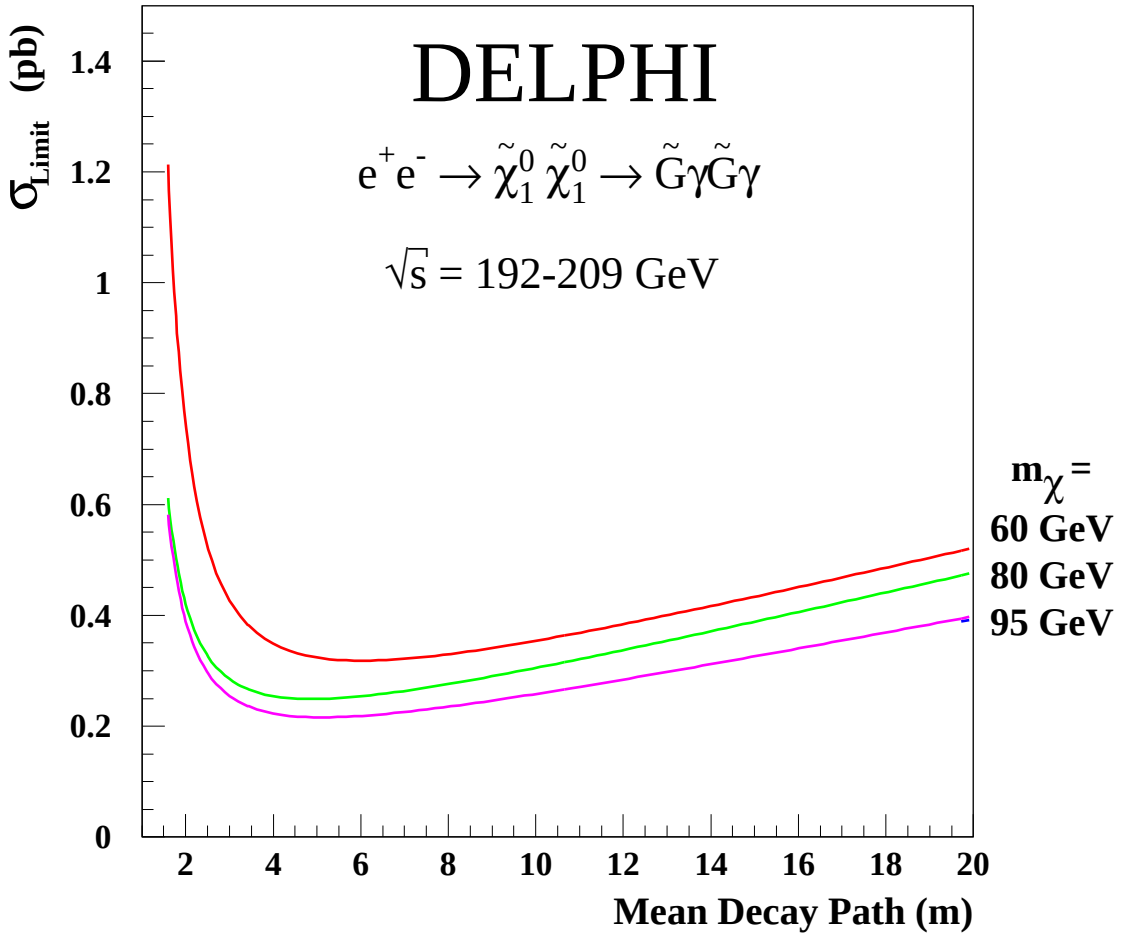

Figure 10: Upper limit at 95% C.L. on the cross-section of the process $e^+e^- \to \tilde{\chi}_1^0\tilde{\chi}_1^0 \to \tilde{G}\gamma\tilde{G}\gamma$ as a function of the $\tilde{\chi}_1^0$ mean decay path for different hypotheses for the neutralino mass. The data collected at $\sqrt{s}$ =192-209 GeV was used to produce this plot.

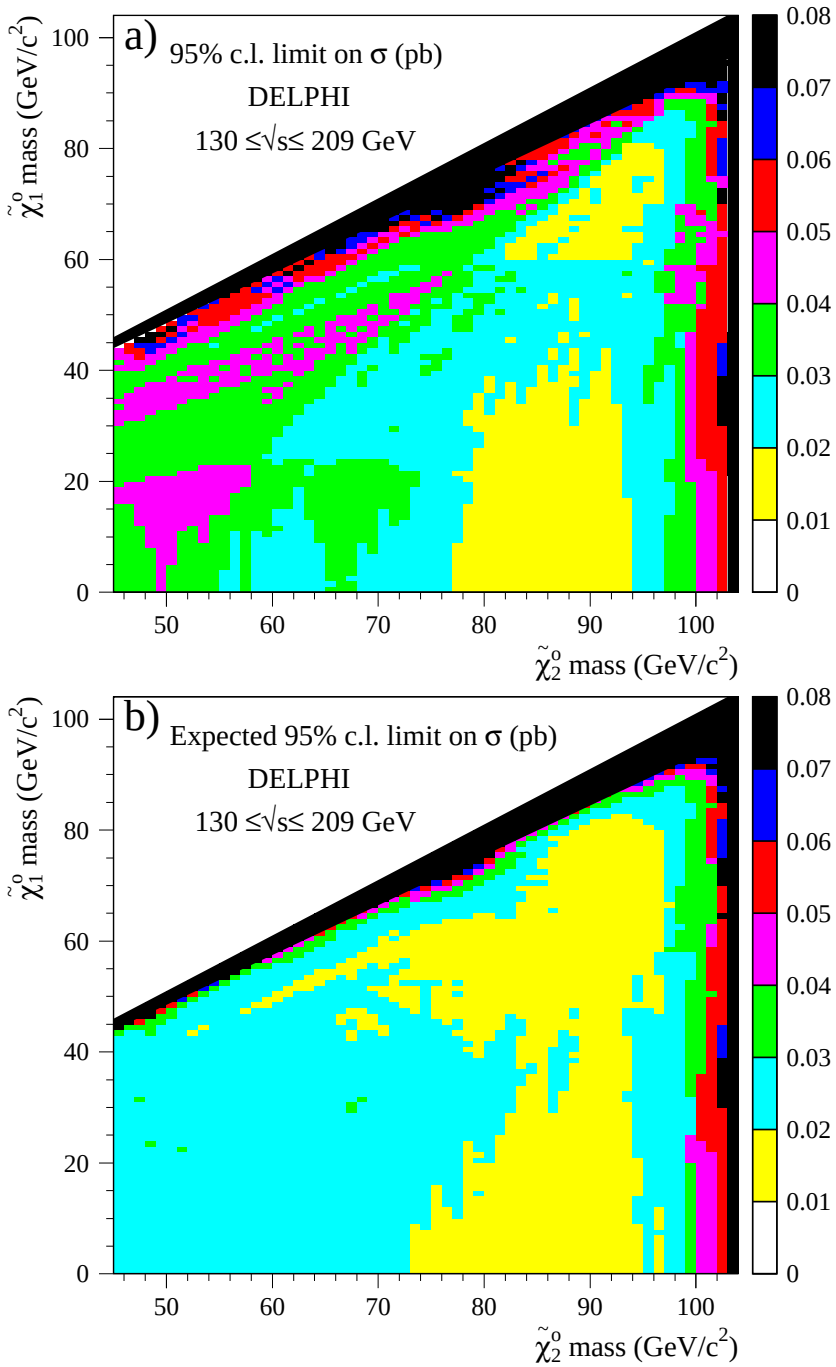

Figure 11: a) The observed upper limit at 95% C.L. on the cross-section at $\sqrt{s}$ =208 GeV of the process $e^+e^- \to \tilde{\chi}_2^0\tilde{\chi}_2^0 \to \tilde{\chi}_1^0\gamma\tilde{\chi}_1^0\gamma$ as a function of the $\tilde{\chi}_1^0$ and the $\tilde{\chi}_2^0$ mass. The different shaded areas correspond to limits in pb as indicated by the shading scale on the right hand side. The limit was obtained by combining the data taken at $\sqrt{s}$ =130-209 GeV, assuming the signal cross-section to scale as β/s. b) The expected upper limit at 95% C.L. on the cross-section at $\sqrt{s}$ =208 GeV of the process $e^+e^- \to \tilde{\chi}_2^0\tilde{\chi}_2^0 \to \tilde{\chi}_1^0\gamma\tilde{\chi}_1^0\gamma$.